Scientific Research Publishing

Energy and Power Engineering, 2024, 16, 313-323
https://www.scirp.org/journal/epe
ISSN Online: 1947-3818
ISSN Print: 1949-243X

Corrective Effect of the Angle of Incidence of the Magnetic Field Intensity on the Performance (Series and Shunt Resistances) of a Bifacial Silicon Solar Cell

Idrissa Sourabié[1], Mahamadi Savadogo[2], Boubacar Soro[2], Ramatou Saré[2], Christian Zoundi[1], Martial Zoungrana[2], Issa Zerbo[2]

[1]Laboratoire de Chimie Analytique, de Physique Spatiale et Énergétique (L@CAPSE), Ecole Doctorale Sciences et Technologies, Université Norbert ZONGO, Koudougou, Burkina Faso
[2]Laboratoire d'Energies Thermiques Renouvelables (L.E.T.RE), Ecole Doctorale Sciences et Technologies, Université Joseph KI-ZERBO, Ouagadougou, Burkina Faso
Email: idmanos45@gmail.com

How to cite this paper: Sourabié, I., Savadogo, M., Soro, B., Saré, R., Zoundi, C., Zoungrana, M. and Zerbo, I. (2024) Corrective Effect of the Angle of Incidence of the Magnetic Field Intensity on the Performance (Series and Shunt Resistances) of a Bifacial Silicon Solar Cell. *Energy and Power Engineering*, **16**, 313-323.
https://doi.org/10.4236/epe.2024.169015

Received: July 10, 2024
Accepted: September 9, 2024
Published: September 12, 2024

Abstract

This article presents a three-dimensional analysis of the impact of the angle of incidence of the magnetic field intensity on the electrical performance (series resistance, shunt resistance) of a bifacial polycrystalline silicon solar cell. The cell is illuminated simultaneously from both sides. The continuity equation for the excess minority carriers is solved at the emitter and at the depth of the base respectively. The analytical expressions for photocurrent density, photovoltage, series resistance and shunt resistance were deduced. Using these expressions, the values of the series and shunt resistances were extracted for different values of the angle of incidence of the magnetic field intensity. The study shows that as the angle of incidence increases, the slopes of the minority carrier density for the two modes of operation of the solar cell decrease. This is explained by a drop in the accumulation of carriers in the area close to the junction due to the fact that the Lorentz force is unable to drive the carriers towards the lateral surfaces due to the weak action of the magnetic field, which tends to cancel out as the incidence angle increases, and consequently a drop in the open circuit photovoltage. This, in turn, reduces the Lorentz force. These results predict that the p-n junction of the solar cell will not heat up. The study also showed a decrease in series resistance as the incidence angle of the magnetic field intensity increased from 0 rad to π/2 rad and an increase in shunt resistance as the incidence angle increased. His behaviour of the electrical parameters when the angle of incidence of the field from 0 rad to π/2 rad

shows that the decreasing magnetic field vector tends to be collinear with the electron trajectory. This allows them to cross the junction and participate in the external current. The best orientation for the Lorentz force is zero, in which case the carriers can move easily towards the junction.

Keywords

Angle of Incidence, Magnetic Field Intensity, Bifacial Polycrystalline Silicon Solar Cell, Series Resistance, Shunt Resistance

1. Introduction

Energy has become a vital issue in today's demographic and industrial boom. To answer this question, many countries have decided to implement energy policies that include renewable energies in their energy consumption. These are wind energy; solar energy; biomass…

Solar energy is the most abundant of these energies, because it comes from the sun. This energy is used to generate electricity from photovoltaic solar cells.

Nowadays, most research is based on improving the efficiency of solar cells in terms of the external factors that influence their operation.

Researchers such as Zerbo *et al.* [1] and many others [2] [3]-[10] have carried out one-dimensional simulation studies of the effect of the magnetic field on bifacial polycrystalline silicon solar cells of the type n^+-p-p^+. In their studies, the authors all considered an orientation of the magnetic field vector parallel to the p-n junction. The study shows that the magnetic field has a detrimental effect on the electronic and electrical performance of photovoltaic solar cells. To find a solution to the effect of the magnetic field, Sourabié *et al.* [11] [12] introduced the concept of the incidence angle of the magnetic field intensity. They investigated the effect of the angle of incidence of the magnetic field intensity on the electrical parameters of monofacial and bifacial solar cells. Their study showed that the impact of the magnetic field intensity could be corrected by orienting the Lorentz force perpendicularly.

His work follows on from that of Sourabié *et al.* [12], investigating the series and shunt resistances of the bifacial photopile illuminated simultaneously from both sides by multtispectral light.

This work is being carried out in three dimensions (3D) to model the effect of the angle of incidence of the magnetic field intensity on the electrical performance (series resistance and shunt) of a bifacial photocell grain illuminated simultaneously from both sides.

To achieve this, we solved the continuity equation manually, while respecting the principles of mathematical calculation, which led to the determination of the expressions for the photovoltage and photocurrent density. Using these expressions, we deduced the series and shunt resistances and then proceeded to represent

the series and shunt resistances as a function of the angle of incidence of the magnetic field intensity using a simulation carried out with mathcad 15 software.

The extracted values are transposed to origin 8 to plot the curves.

2. Methods and Theories

2.1. Excess Minority Carriers Density

This study was carried out on an n^+-p-p^+ type polycrystalline silicon bifacial solar cell grain. It should be noted that the solar cell grain has the same electrical properties (doping rate, mobility of minority carriers, lifetime and diffusion length) as a polycrystalline silicon PV cell. This is because studies have shown that the PV cell is made up of an association of pieces of very small single crystals separated by transition zones called grain boundaries [13]-[15]. These transition zones are therefore major centres of recombination. For modelling purposes, we assume that the grain boundaries are perpendicular to the front and back surfaces, and therefore; at the junction. Also, the perturbation (injection of carriers) applied to the base of the grain is not very intense so as to modify the mobility of the free electrons, so the crystalline field in the base is not taken into account.

The value of the emitter of the photopile grain is H = 0.03 cm and those of the diffusion length and diffusion coefficient are: Ln = 0.015 cm; Dn = 26 cm^2/s. In order to simplify the expressions for minority carrier density and photocurrent density, photovoltage, series and shunt resistance, we have assumed a square cross-section for the grains. The analysis can then be extended to a parallelepiped grain shape [16].

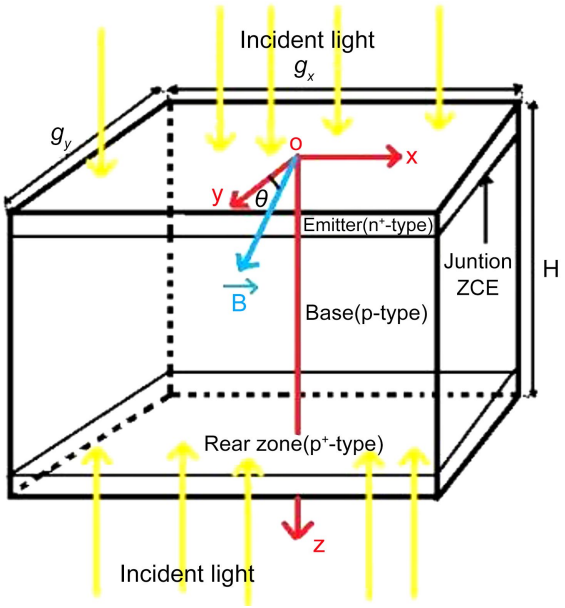

Figure 1. Grain of bifacial polycrystalline silicon solar cell illuminated by multispectral light and under the influence of incidence angle of magnetic field.

When the photopile grain, placed in a region where the magnetic field is constant (B = 7.5 mT) and makes an angle θ with the Oy axis, is simultaneously illuminated from both sides with multispectral light (**Figure 1**) and the light penetrates along the (Oz) axis as well as generating excess minority charge carriers, the transport phenomena are governed by the continuity equation [11] [12].

$$\frac{\partial^2\delta(x,y,z)}{\partial x^2}+C_y\cdot\frac{\partial^2\delta(x,y,z)}{\partial y^2}+\left[1+\left(\mu_n B_0\sin\theta\right)^2\right]\frac{\partial^2\delta(x,y,z)}{\partial z^2}-\frac{\delta(x,y,z)}{L_n^{*2}}=-\frac{G(z)}{D_n^*} \tag{1}$$

$$C_y=\left[1+\left(\mu_n B_0\sin\theta\right)^2\right],\quad D_n^*=\frac{D_n}{1+\left(\mu_0 B_0\right)^2}\quad\text{and}\quad L_n^*=\frac{L_n}{1+\left(\mu_0 B_0\right)^2}$$

The general solution to the continuity equation is [11]:

$$\delta(x,y,z)=\sum_j^\infty\sum_k^\infty\left[A_{j,k}\cosh\left(\frac{z}{L_{j,k}}\right)+B_{j,k}\sinh\left(\frac{z}{L_{j,k}}\right)-\sum_{i=1}^3 K_i\left[\mathrm{e}^{-b_i z}+\mathrm{e}^{-b_i(H-z)}\right]\right] \tag{2}$$

$$K_i=\frac{n\cdot a_i\cdot L_{j,k}^2}{D_{j,k}\cdot\left[\left(b_i\cdot L_{j,k}\right)^2-1\right]} \tag{3}$$

The coefficients $A_{j,k}$ and $B_{j,k}$ are fully determined using the boundary conditions at the junction and at the back of the solar cell [11] [15] [16]. In this way, the expression for the density of minority charge carriers will be completely determined.

2.2. Photocurrent Density

By applying Fick's law to the junction of the bifacial cell grain, we obtain the expression for the photocurrent density given by Equation (3):

$$J_{Ph}(Sf,B,\theta)=e\cdot D(\theta)\sum_j\sum_k R_{jk}\left[\frac{B_{jk}}{L_{jk}}+\sum_{i=1}^3 K_i\cdot b_i\left(1+\mathrm{e}^{-b_i\cdot H}\right)\right] \tag{4}$$

This expression has two significant variables: the dynamic velocity at the junction Sf and the angle of incidence of the magnetic field intensity.

2.3. Photovoltage

The expression for the photovoltage (Equation (4)) across the bifacial cell junction is obtained using the Boltzmann approximation.

$$V_{ph}(Sf,B,\theta)=V_T\cdot\ln\left[1+\frac{1}{n_0}\sum_j\sum_k R_{jk}\cdot\left[A_{jk}-\sum_{i=1}^3 K_i\left(1+\mathrm{e}^{-b_i H}\right)\right]\right] \tag{5}$$

with V_T the thermal voltage with value V_T = 26 mV; n_o is the electron density at thermodynamic equilibrium.

3. Cell Performance Parameters

The performance parameters (shunt and series resistances) of the bifacial cell

grain are electrical parameters that can be used to judge the performance of a cell.

3.1. Series Resistance

The expression for series resistance is given by Equation (5).

$$R_s\left(Sf,B,\theta\right)=\frac{V_{co}\left(B,\theta\right)-V_{ph}\left(Sf,B,\theta\right)}{J_{ph}\left(Sf,B,\theta\right)} \tag{6}$$

3.2. Shunt Resistance

The expression for the shunt resistance is given in Equation (6).

$$R_{sh}\left(Sf,B,\theta\right)=\frac{V_{ph}\left(Sf,B,\theta\right)}{J_{phcc}-J_{ph}\left(Sf,B,\theta\right)} \tag{7}$$

4. Results and Discussion

From Equations (2); (5) and (6) above, we discuss the impact of the angle of incidence of the magnetic field strength on the performance of the bifacial photocell grain. This analysis is possible thanks to the variations in series and shunt resistances shown in the figures below.

4.1. Effect of the Angle Incidence on the Density of Minority Charge Carriers

Figure 2 shows the profiles of the density of excess minority charge carriers as a function of depth for different values of the angle of incidence of the magnetic field.

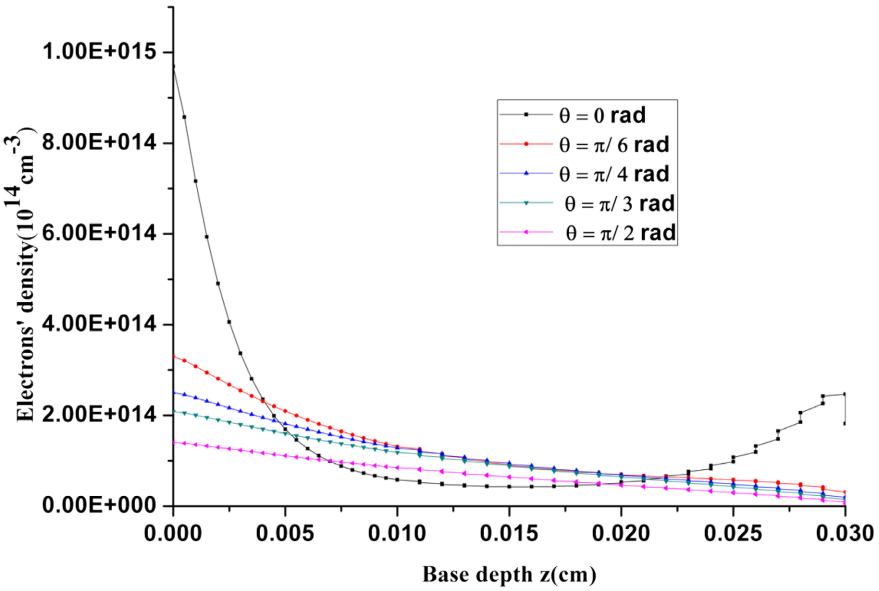

Figure 2. Open-circuit carrier density for different values of angle of incidence (Sf= 0 cm/s; g_x = g_y = 0.003 cm; S_{gb} = 100 cm/s; S_b = 1000 cm/s; L = 0.015 cm; H = 0.03 cm; D_n = 26 cm^2/s; μ_n = 1000 cm^2/V·s).

Simulations are carried out for two types of operation of the solar cell: open-circuit operation (low values of the dynamic speed at the junction) and short-circuit operation (high values of the dynamic speed at the junction).

Figure 2 shows negative slopes at the junction and a maximum at the back when the magnetic field is intense, *i.e.* for $\theta = 0$ rad. In addition, the carrier density decreases as the angle of incidence increases. Figure 2 also shows that after a depth of 0.020 cm the curves are curved. These curvatures are due to the contribution of the rear face of the solar cell grain. The decrease in the carrier density with the increase in the angle of incidence of the magnetic field leads to a drop in the open circuit voltage and therefore a drop in the series resistance.

Figure 3 below shows the carrier density profiles for different values of the angle of incidence of the magnetic field. We also observe a decrease in carrier density as the angle of incidence of the magnetic field increases. The profiles in Figure 3 show peaks justifying the presence of carriers on the front and back of the solar cell. This is justified by the Lorentz force, which reflects the photocarriers back towards the junction and onto the photovoltaic cell interfaces.

Then we see in this Figure 3 that as the angle of incidence of the magnetic field increases, the maxima of the carrier densities between 0.01 cm and 0.02 cm decrease and become linear, thus justifying that the charge carriers photocreated in the base are less present because they have recombined [11] [12].

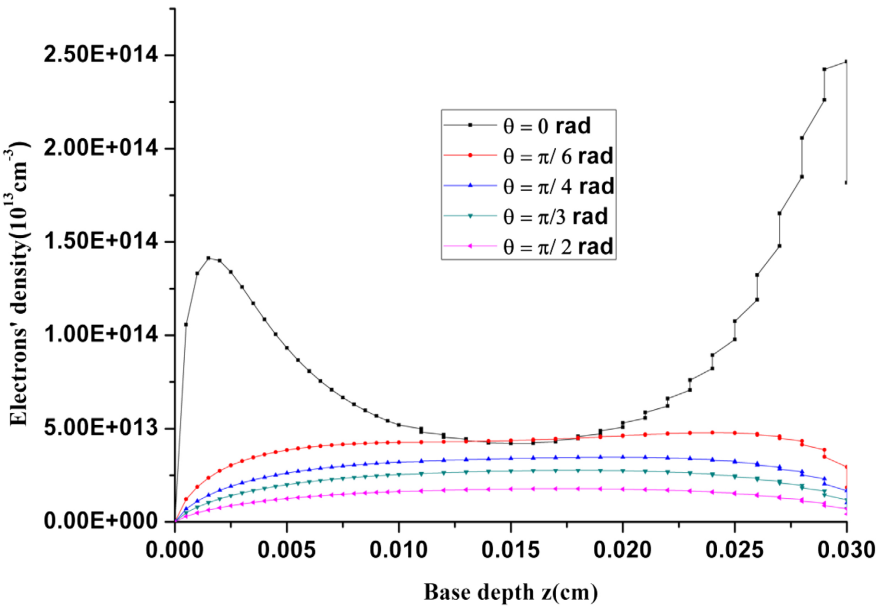

Figure 3. Carrier density in the circuit for different values of the angle of incidence ($Sf = 8 \times 10^8$ cm/s; $g_x = g_y = 0.003$ cm; $S_{gb} = 100$ cm/s; $S_b = 1000$ cm/s; $L = 0.015$ cm; $H = 0.03$ cm; $D_n = 26$ cm^2/s; $\mu_n = 1000$ cm^2/V·s).

4.2. Impact of Angle of Incidence on J-V Characteristics

Figure 4 shows the profiles of photocurrent density versus photovoltage for different values of the angle of incidence of the magnetic field intensity.

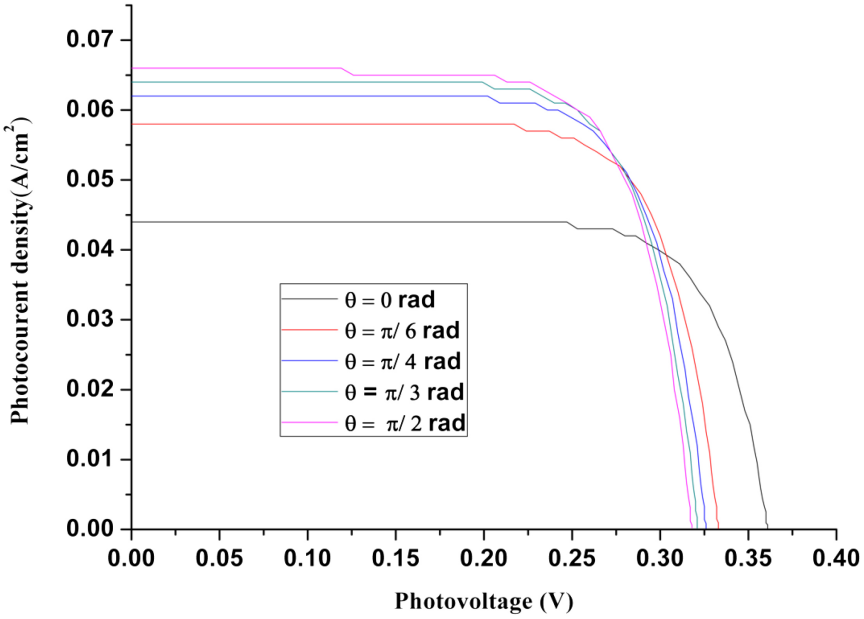

Figure 4. Photocurrent density as a function of photovoltage for different values of angle of incidence (Sf = 0 cm/s; $g_x = g_y$ = 0.003 cm; S_{gb} = 100 cm/s; S_b = 1000 cm/s; L = 0.015 cm; H = 0.03 cm; D_n = 26 cm²/s; μ_n = 1000 cm²/V·s).

Analysis of the curves in **Figure 4** shows that when the angle of incidence varies from 0 to π/2 rad the short-circuit photocurrent density increases and the open-circuit voltage decreases.

Phenomenon observed in **Figure 4**. The increase in photocurrent density and the decrease in open circuit voltage can be explained by the fact that when the angle of incidence increases, the Lorentz force that sends the carriers back towards the lateral faces decreases until it is cancelled, causing the migration of the carriers towards the junction that cross it without being accumulated too much [12].

4.3. Effect of Incidence Angle on Series Resistance

The series resistance is associated with the manufacture of the solar cell. It characterises the loss of carriers at the junction [7]. The higher the resistance, the fewer carriers pass through the junction. As a result, the junction heats up. It is therefore important to minimise it.

Figure 5 shows the variation in series resistance as a function of the angle of incidence of the magnetic field. This variation is periodic with period π.

Figure 5 shows that the series resistance decreases over the interval [0, π/2] and on [π, 3π/2] while the series resistance increases as the angle of incidence varies from π/2 rad of π rad and to 3π/2 rad of 2π rad. So the series resistance as a function of the angle of incidence of the magnetic field is a positive sinusoidal function with period π. Studies have shown that series resistance increases as the magnetic field increases [7]. But in **Figure 5** we can see that it decreases over the interval [0, π/2]. This is because for the angle of incidence varying from 0 to π/2 rad the magnetic field vector tends to be collinear with the carrier velocity vector and the

Lorentz force that deflects the minority carriers photogenerated in the base of the solar cell decreases until it is cancelled out. This encourages the carriers to migrate towards the junction in order to cross it and participate in the external current.

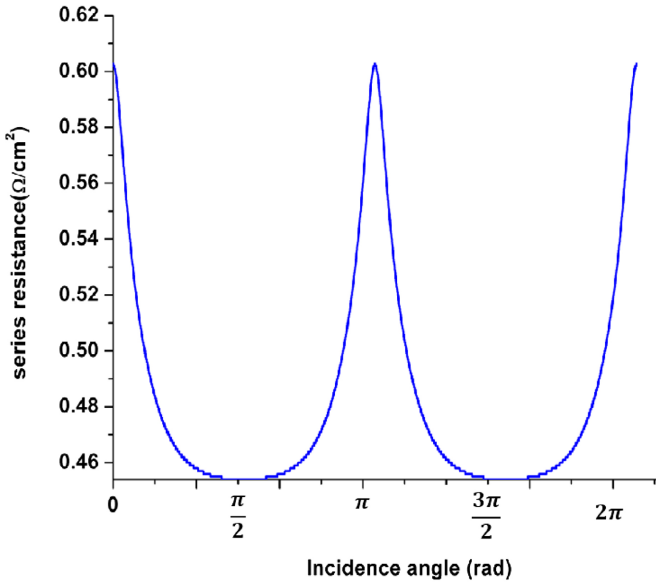

Figure 5. Series resistance as a function of angle of incidence (Sf = 0 cm/s; $g_x = g_y$ = 0.003 cm; S_{gb} = 100 cm/s; S_b = 1000 cm/s; L = 0.015 cm; H = 0.03cm; D_n = 26 cm²/s; μ_n = 1000 cm²/V·s).

4.4. Effect of Incidence Angle on Shunt Resistance

Figure 6 shows the variation in shunt resistance as a function of the angle of incidence of the magnetic field.

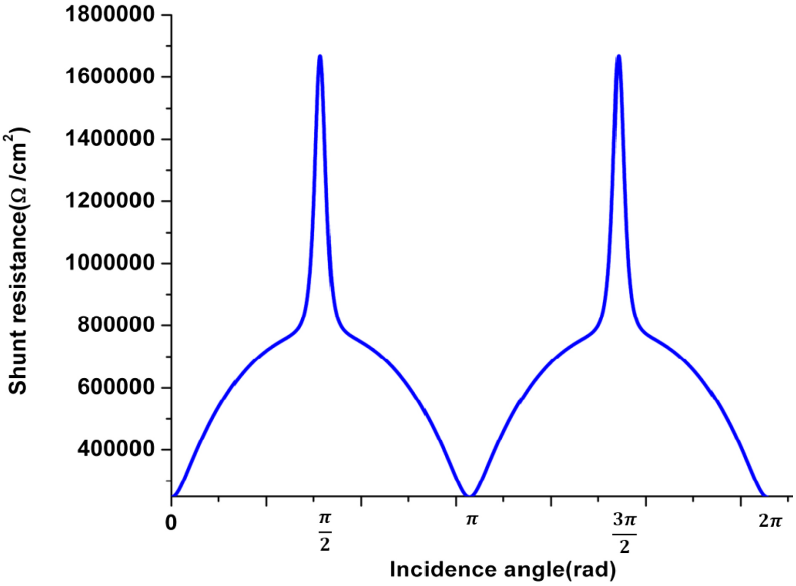

Figure 6. Shunt resistance as a function of incidence angle (Sf = 0 cm/s; $g_x = g_y$ = 0.003 cm; S_{gb} = 100 cm/s; S_b = 1000 cm/s; L = 0.015 cm; H = 0.03cm; D_n = 26 cm²/s; μ_n = 1000 cm²/V·s).

We can see that the shunt resistance increases from 0 to π/2 rad and π rad of 3π/2 rad then decreases π/2 rad of π rad and 3π/2 rad of 2π rad. For values of the angle of incidence equal to π/2 rad of 3π/2 rad the shunt resistance reaches its peak. This is because at these values the Lorentz force has no effect on the movement of the carriers because the magnetic field vector is collinear with the electron velocity vector.

In short, we have shown that when the angle of incidence increases from 0 to π/2 rad of

π rad to 3π/2 rad, the magnetic field tends to cancel out, as does the Lorentz force, resulting in little deflection of the carriers towards the side surfaces of the cell. As a result, there is less loss of carriers at the junction. The increase in the shunt resistance curves with the angle of incidence of the magnetic field from 0 to π/2 rad and π rad of 3π/2 rad is due to the disturbing effect caused by the magnetic field. This is because we expected a decrease in the shunt resistance for the angle of incidence varying from 0 to π/2 rad and π rad of 3π/2 rad.

Table 1 shows that as the angle of incidence of the magnetic field intensity increases, the values of the series resistance decrease while those of the shunt resistance increase. This is the result of the decrease in voltage at the junction due to the Lorentz force, which tends to cancel out. Hence the strong migration of carriers across the junction.

Table 1. Shows the electrical performance of the solar cell obtained during the simulation.

θ (rad)	Series resistance ($\Omega \cdot cm^2$)	Shunt resistance ($\Omega \cdot cm^2$)
0	0.603	2.476×10^5
π/6	0.481	5.504×10^5
π/4	0.464	6.589×10^5
π/3	0.457	7.289×10^5
π/2	0.454	16.68×10^5

5. Conclusions

An analysis of the impact of the angle of incidence of the magnetic field intensity on the electrical performance of a bifacial photocell under multispectral illumination from both sides. This three-dimensional model shows a decrease in the densities of excess minority charge carriers, photovoltage and series resistance, and an increase in photocurrent density and shunt resistance when the angle of incidence of the magnetic field increases by 0 rad to π/2 rad.

The results show that the degradation in solar cell performance induced by the application of a magnetic field can be reduced by increasing the incidence angle. The results, therefore, show that when PV modules are installed, they should be tilted so that the magnetic field lines form an angle of θ with the junction of the solar cell.

The behaviour of the shunt resistance as the angle of incidence increases would be due to the disturbance induced by the magnetic field strength. So, this increase in shunt resistance with the incidence angle could be beneficial to the p-n junction of the solar cell. Because a low shunt resistance can considerably affect the performance of a PV cell.

Acknowledgements

The authors are grateful to International Science Program (ISP) for supporting their research group (energy and environment) and allowing them to conduct this work.

Conflicts of Interest

The authors declare no conflicts of interest regarding the publication of this paper.

References

[1] Zerbo, I., Zoungrana, M., Sourabie, I., Ouedraogo, A., Zouma, B. and Bathiebo, D.J. (2015) External Magnetic Field Effect on Bifacial Silicon Solar Cell's Electric Power and Conversion Efficiency. *Turkish Journal of Physics*, **39**, 288-294. https://doi.org/10.3906/fiz-1505-10

[2] Zoungrana, M., Zerbo, I., Ouédraogo, F., Zouma, B. and Zougmoré, F. (2012) 3D Modelling of Magnetic Field and Light Concentration Effects on a Bifacial Silicon Solar Cell Illuminated by Its Rear Side. *IOP Conference Series: Materials Science and Engineering*, **29**, Article 012020. https://doi.org/10.1088/1757-899x/29/1/012020

[3] Mbodji, S., Zoungrana, M., Zerbo, I., Dieng, B. and Sissoko, G. (2015) Modelling Study of Magnetic Field's Effects on Solar Cell's Transient Decay. *World Journal of Condensed Matter Physics*, **5**, 284-293. https://doi.org/10.4236/wjcmp.2015.54029

[4] Zerbo, I., Zoungrana, M., Sourabié, I., Ouedraogo, A., Zouma, B. and Bathiebo, D.J. (2016) External Magnetic Field Effect on Bifacial Silicon Solar Cell's Electrical Parameters. *Energy and Power Engineering*, **8**, 146-151. https://doi.org/10.4236/epe.2016.83013

[5] Kooffreh, M.E., Udensi, O.U. and Umoeyen, A.J. (2017) Modifying and Adapting a Plant-Based DNA Extraction Protocol for Human Genomic DNA Extraction: A Cost Effective Approach. *Global Journal of Pure and Applied Sciences*, **23**, 1-4. https://doi.org/10.4314/gjpas.v23i1.1

[6] Zoungrana, M., Zerbo, I., Soro, B., Sawadogo, M., Tiendrebeogo, S. and Bathiebo, D.J. (2017) The Effect of Magnetic Field on the Efficiency of a Silicon Solar Cell under an Intense Light Concentration. *Advances in Science and Technology Research Journal*, **11**, 133-138.

[7] Combari, D.U., Ramde, E.W., Sourabie, I., Zoungrana, M., Zerbo, I. and Bathiebo, D.J. (2018) Performance Investigation of a Silicon Photovoltaic Module under the Influence of a Magnetic Field. *Advances in Condensed Matter Physics*, **2018**, 1-8. https://doi.org/10.1155/2018/6096901

[8] Combari, D.U., Ramde, E.W., Korgo, B., Saré, R., Zoungrana, M. and Zerbo, I. (2021) Investigating the Effect of Inclination Angle of Magnetic Field Vector on Silicon PV Modules. *International Journal of Photoenergy*, **2021**, 1-6. https://doi.org/10.1155/2021/8818869

[9] Erel, S. (2002) The Effect of Electric and Magnetic Fields on the Operation of a Photovoltaic Cell. *Solar Energy Materials and Solar Cells*, **71**, 273-280. https://doi.org/10.1016/s0927-0248(01)00088-5

[10] Betser, Y., Ritter, D., Bahir, G., Cohen, S. and Sperling, J. (1995) Measurement of the Minority Carrier Mobility in the Base of Heterojunction Bipolar Transistors Using a Magnetotransport Method. *Applied Physics Letters*, **67**, 1883-1884. https://doi.org/10.1063/1.114364

[11] Sourabié, I., Zerbo, I., Zoungrana, M., Combari, D.U. and Bathiebo, D.J. (2017) Effect of Incidence Angle of Magnetic Field on the Performance of a Polycrystalline Silicon Solar Cell under Multispectral Illumination. *Smart Grid and Renewable Energy*, **8**, 325-335. https://doi.org/10.4236/sgre.2017.810021

[12] Sourabié, I., Barandja, V.d.D.B., Savadogo, M., Konaté, R., Gnabahou, A.D., Zoungra, M., *et al.* (2022) Three-dimensional Study of the Effect of the Angle of Incidence of a Magnetic Field on the Electrical Power and Conversion Efficiency of a Polycrystalline Silicon Solar Cell under Multispectral Illumination. *Smart Grid and Renewable Energy*, **13**, 295-304. https://doi.org/10.4236/sgre.2022.1312018

[13] Ba, B. and Kane, M. (1995) Open-Circuit Voltage Decay in Polycrystalline Silicon Solar Cells. *Solar Energy Materials and Solar Cells*, **37**, 259-271. https://doi.org/10.1016/0927-0248(95)00019-4

[14] Dugas, J. (1994) 3D Modelling of a Reverse Cell Made with Improved Multicrystalline Silicon Wafers. *Solar Energy Materials and Solar Cells*, **32**, 71-88. https://doi.org/10.1016/0927-0248(94)90257-7

[15] Priester, L. (1980) Approche géométrique des joints de grains. Intérêt et limite. *Revue de Physique Appliquée*, **15**, 789-830. https://doi.org/10.1051/rphysap:01980001504078900

[16] Saré, R., Saria, M., Combari, D.U., Sourabié, I., Barandja, V.D.D.B., Zoungrana, M. and Zerbo, I. (2023) 3D Modelling of the Effects of Electrons Losses at the Junction of a Polycrystalline Silicon PV Cell on Its Performance. *International Journal of Innovation and Applied Studies*, **40**, 1515-1530. http://www.ijias.issr-journals.org/